



**HAL**  
open science

## Chitosan as an antioxidant alternative to sulphites in oenology: EPR investigation of inhibitory mechanisms

Antonio Castro Marín, Marcel Culcasi, Mathieu Cassien, Pierre Stocker, Sophie Thétiot-Laurent, Bertrand Robillard, Fabio Chinnici, Sylvia Pietri

### ► To cite this version:

Antonio Castro Marín, Marcel Culcasi, Mathieu Cassien, Pierre Stocker, Sophie Thétiot-Laurent, et al.. Chitosan as an antioxidant alternative to sulphites in oenology: EPR investigation of inhibitory mechanisms. Food Chemistry, 2019, 10.1016/j.foodchem.2019.01.155 . hal-02004026

**HAL Id: hal-02004026**

**<https://amu.hal.science/hal-02004026>**

Submitted on 1 Feb 2019

**HAL** is a multi-disciplinary open access archive for the deposit and dissemination of scientific research documents, whether they are published or not. The documents may come from teaching and research institutions in France or abroad, or from public or private research centers.

L'archive ouverte pluridisciplinaire **HAL**, est destinée au dépôt et à la diffusion de documents scientifiques de niveau recherche, publiés ou non, émanant des établissements d'enseignement et de recherche français ou étrangers, des laboratoires publics ou privés.



Distributed under a Creative Commons Attribution 4.0 International License

## Accepted Manuscript

Chitosan as an antioxidant alternative to sulphites in oenology: EPR investigation of inhibitory mechanisms

Antonio Castro Marín, Marcel Culcasi, Mathieu Cassien, Pierre Stocker, Sophie Thétiot-Laurent, Bertrand Robillard, Fabio Chinnici, Sylvia Pietri

PII: S0308-8146(19)30230-4

DOI: <https://doi.org/10.1016/j.foodchem.2019.01.155>

Reference: FOCH 24250

To appear in: *Food Chemistry*

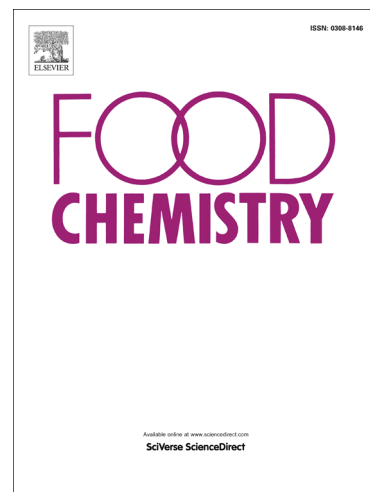
Received Date: 20 September 2018

Revised Date: 21 January 2019

Accepted Date: 22 January 2019

Please cite this article as: Castro Marín, A., Culcasi, M., Cassien, M., Stocker, P., Thétiot-Laurent, S., Robillard, B., Chinnici, F., Pietri, S., Chitosan as an antioxidant alternative to sulphites in oenology: EPR investigation of inhibitory mechanisms, *Food Chemistry* (2019), doi: <https://doi.org/10.1016/j.foodchem.2019.01.155>

This is a PDF file of an unedited manuscript that has been accepted for publication. As a service to our customers we are providing this early version of the manuscript. The manuscript will undergo copyediting, typesetting, and review of the resulting proof before it is published in its final form. Please note that during the production process errors may be discovered which could affect the content, and all legal disclaimers that apply to the journal pertain.



# Chitosan as an antioxidant alternative to sulphites in oenology: EPR investigation of inhibitory mechanisms

Antonio Castro Marín<sup>a,b</sup>, Marcel Culcasi<sup>a,\*</sup>, Mathieu Cassien<sup>a</sup>, Pierre Stocker<sup>a</sup>,

Sophie Thétiot-Laurent<sup>a</sup>, Bertrand Robillard<sup>c</sup>, Fabio Chinnici<sup>b</sup>, Sylvia Pietri<sup>a</sup>

Addresses: <sup>a</sup> Aix Marseille Univ, CNRS, ICR, Marseille, France.

<sup>b</sup> Department of Agricultural and Food Sciences, University of Bologna, Bologna, Italy.

<sup>c</sup> Institut Oenologique de Champagne, Epernay, France.

Corresponding author: Marcel CULCASI, PhD

Institut de Chimie Radicalaire, Sondes Moléculaires en Biologie et Stress Oxydant,

Aix Marseille Université, CNRS UMR 7273

Centre scientifique de Saint Jérôme, Avenue Escadrille Normandie Niemen, Service 522

13397 Marseille cedex 13, France

Tel: 00 33 (0)4 91 28 90 25

e-mail: marcel.culcasi@univ-amu.fr

**Abstract**

The efficacy against oxidative degradation in model and sulphite-free white wines of two commercial, insoluble chitosans (one being approved for winemaking) were investigated by electron paramagnetic resonance (EPR). Both compounds at various doses significantly inhibited the formation of  $\alpha$ -(4-pyridyl-1-oxide)-*N*-*t*-butylnitrone (4-POBN)-1-hydroxyethyl adducts under normal wine storage conditions. Pre-incubation with 2 g/L chitosan followed by filtration had a better effect than adding 50 mg/L sulphur dioxide to the experimental Chardonnay wine on the release of 4-POBN adducts after 6 days of incubation with 100  $\mu$ M iron(II). In a relevant photooxidative system acetaldehyde formation was significantly reduced after 6 days of incubation. Parallel EPR tests were performed to assess the importance of metal chelation (iron and copper) versus direct scavenging of hydroxyl radicals on the effect of chitosan. The present data support the potentiality of using biocompatible chitosan as a healthier complement and/or alternative to sulphur dioxide against white wine oxidative spoilage.

**Keywords:** Antioxidant, Chitosan, EPR spin trapping, Hydroxyl radical scavenging activity, Metal chelation, Photooxidation, Sulphur dioxide-free wines

**Abbreviations:** AAPH, 2,2'-azobis(2-methylpropionamide) dihydrochloride; CHI, chitosan; DAD, diode array detection; DEPMPO; 5-(diethoxyphosphoryl-5-methyl)-1-pyrroline-*N*-oxide; DNPH, 2,4-dinitrophenylhydrazine; DMPO, 5,5'-dimethyl-1-pyrroline-*N*-oxide; EPR, Electron paramagnetic resonance; H<sub>2</sub>O<sub>2</sub>, hydrogen peroxide; 1-HER, 1-hydroxyethyl radical; 4-MeC, 4-methylcatechol; PBS, phosphate-buffered saline; 4-POBN,  $\alpha$ -(4-pyridyl-1-oxide)-*N*-*t*-butylnitrone; ORAC, oxygen radical absorbance capacity.

ACCEPTED MANUSCRIPT

## 1. Introduction

Skilled oxidation management is perhaps the most crucial task in winemaking since it can offer significant improvement of the organoleptic characteristics (color, flavors and taste) and shelf life of the finished wine. In the last decades a vast literature has arisen dealing with the molecular events behind non-enzymatic oxidation of wine (Danilewicz, 2003; Oliveira, Ferreira, De Freitas & Silva, 2011; Waterhouse & Laurie, 2006) that would guide technological interventions in wineries. The most plausible scenario for wine oxidation globally resembles that of oxidative stress in biology but, unlike in respiring cells, molecular oxygen is here reduced to water univalently, with successive formation of the hydroperoxyl radical  $\text{HOO}\bullet$  (the protonated form of superoxide ( $\text{O}_2\bullet^-$ ) at wine pH), hydrogen peroxide ( $\text{H}_2\text{O}_2$ ), and finally the hydroxyl radical ( $\text{HO}\bullet$ ). This cascade of reactions are susceptible to occur at any stage of winemaking, including after bottling, since the volume of dissolved oxygen and the headspace above the wine can reach several mL depending on type of closure and adopted vinification technology (Grant-Preece, Barril, Schmidtke & Clark, 2017). This results in oxidation of the wine polyphenols to corresponding *o*-quinones and brown pigments (a phenomenon called 'browning'), with undesired effects on the aromatic profile and color (Oliveira et al., 2011; Waterhouse & Laurie, 2006). Trace transition metals, particularly iron and copper, have been shown to play a cardinal role in wine oxidation, notably because they catalyze the reduction of  $\text{H}_2\text{O}_2$  to  $\text{HO}\bullet$  by a Fenton-type reaction, being then redox cycled by those polyphenols, with experiments often involving the representative compound 4-methylcatechol (4-MeC), not itself found in wine but bearing a typical catechol moiety (Danilewicz, 2003). Finally,  $\text{HO}\bullet$  will oxidise ethanol and tartaric acid to acetaldehyde  $\text{CH}_3\text{CHO}$  and glyoxylic acid, respectively, the former imparting to white wine a characteristic oxidative odor upon accumulation.

Of the available methodologies to study the reactivity of HO• in wine oxidation, electron paramagnetic resonance (EPR) spectroscopy coupled to spin-trapping has led to conclusive advances in the understanding of free radical processes. Fig. 1 shows that hydroxyl radicals, which nonspecifically attack any molecule at diffusion controlled rates (i.e., with second-order rate constants  $> 10^9 \text{ M}^{-1} \cdot \text{s}^{-1}$ ), will oxidise ethanol to the main, thermodynamically stabilized secondary 1-hydroxyethyl radical (1-HER) intermediate. In low O<sub>2</sub> conditions 1-HER is readily oxidized by Fe(III) to yield acetaldehyde. Despite being quenched by many wine constituents such as polyphenols and thiols (Kreitman, Laurie & Elias, 2013) enough 1-HER remains available to be spin trapped on nitrones added to a wine oxidation system, giving nitroxide adducts that can sometimes be detected for days (Elias, Andersen, Skibsted & Waterhouse, 2009a, 2009b; Elias & Waterhouse, 2010; Kreitman, Cantu, Waterhouse & Elias, 2013; Zhang, Shen, Fan, García Martín, Wang & Song, 2015; Nikolantonaki et al., 2019).

In oenology the most widely used intervention to protect must and wine against oxidation and microbial activity is adding sulphur dioxide (SO<sub>2</sub>). Bisulfite, the active form of SO<sub>2</sub> at wine pH, is presumed to lessen overall wine oxidation process at several stages, i.e., by scavenging H<sub>2</sub>O<sub>2</sub> to yield sulfate (Fig. 1), reducing *o*-quinones back to their phenolic precursors, or binding to carbonyls, especially the most abundant one, acetaldehyde (Danilewicz, 2003; Oliveira et al., 2011). Despite their remarkable efficacy, simple implementation and low cost, however, sulphites have demonstrated latent adverse effects in hypersensitive individuals, e.g., they may aggravate the symptoms of allergic asthma (Vally, Misso & Madan, 2009), and there is movement to promote supposedly healthier non-sulphited wines, or to support antioxidant alternatives in winemaking. Most if not all of the new technologies (pulsed electric fields, ultrasounds, UV irradiation) and natural preservation chemicals (dimethyl dicarbonate, lysozyme, bacteriocins) under development have as their purpose antimicrobial and enzyme inactivating effects (Santos,

Nunes, Saraiva & Coimbra, 2012). Furthermore, the use of other additives such as glutathione, ascorbic acid or polyphenols intended at inhibiting free radical mediated wine oxidation at H<sub>2</sub>O<sub>2</sub> stage or downstream remain marginal (Kemp, Alexandre, Robillard & Marchal, 2015).

Another attractive route to control wine oxidation is inactivation of catalytic metals by potent chelators, as such intervention would, in principle, simultaneously inhibit Fenton chemistry, and the formation of *o*-quinones and acetaldehyde (Fig. 1). Chitosan is a  $\beta$ -1.4-connected linear polymer of D-glucosamine usually obtained by deacetylation of chitin, a homopolymer of *N*-acetyl glucosamine extracted from insects, crustaceans or fungi. Due to its regular and high density of amino and hydroxy groups (Fig. 1), this non-toxic, biodegradable biopolymer has remarkable metal chelation power and, because of its polycationic nature, chitosan also exhibits anti-microbial activity, both properties having attracted food scientists for decades (Bornet & Teissedre, 2008). Moreover, use of chitosan as an additive in winemaking for preventing cloudiness, removal of heavy metals, and reduction of *Brettanomyces spp.* contamination has been regulated by the EU in 2011 (EC Regulation No 53/2011). Since its early introduction as anti-browning agent in white wines (Spagna, Pifferi, Rangoni, Mattivi, Nicolini & Palmonari 1996) chitosan has stimulated wine researchers as a substitute for SO<sub>2</sub> (Chinnici, Natali & Riponi, 2014) and is gaining popularity in winemaking (Colangelo, Torchio, De Faveri & Lambri, 2018; Filipe-Ribeiro, Cosme & Nunes, 2018; Castro-Marín, Buglia, Riponi & Chinnici, 2018). In the present work established EPR spin trapping and wine oxidation relevant techniques were applied for the first time, to obtain a deeper understanding of the mechanisms of how an approved, insoluble chitosan protects against white wine spoilage in winemaking conditions.

## 2. Materials and methods

### 2.1. Chemicals and wine samples

The spin traps  $\alpha$ -(4-pyridyl-1-oxide)-*N*-*t*-butyl nitron (4-POBN) and 5,5'-dimethyl-1-pyrroline-*N*-oxide (DMPO) were from TCI (Zwijndrecht, Belgium), and 5-(diethoxyphosphoryl-5-methyl)-1-pyrroline-*N*-oxide (DEPMPO) was synthesized and purified as reported (Culcasi, Rockenbauer, Mercier, Clément & Pietri, 2006). Fluorescein, 6-hydroxy-2,5,7,8-tetramethylchromane-2-carboxylic acid (Trolox) and 2,2'-azobis(2-methylpropionamide) dihydrochloride (AAPH) were from Acros (Illkirch, France). Phosphate-buffered saline (PBS) and other solvents or chemicals, including ferric chloride, ferrous sulfate heptahydrate, copper(II) sulfate, ferrozine [4,4'-[3-(2-pyridinyl)-1,2,4-triazine-5,6-diyl]bisbenzenesulphonic acid], 2,4-dinitrophenylhydrazine (DNPH), 4-MeC, potassium metabisulfite, (+)-tartaric acid, acetaldehyde, and H<sub>2</sub>O<sub>2</sub> were of analytical (> 98.5%) or HPLC grade from Sigma-Aldrich (Saint-Quentin Fallavier, France). Doubly distilled deionized water was used throughout.

A 75–85% deacetylated chitosan having a 50–190 kDa molecular weight was purchased from Sigma-Aldrich (CHI-1; product 448869), and a 80–90% deacetylated chitosan having an average molecular weight of 10–30 kDa (CHI-2) of fungal origin (*Aspergillus niger*) obtained from KitoZyme (Herstal, Belgium) were studied.

Commercially available sulphur dioxide-free white wine samples, obtained from Chardonnay grapes (100%; AOP Coteaux Champenois), were kindly provided by Champagne J. de Telmont (Damery, France). These wines had the following oenological characteristics, measured according to standard procedures described in the 'Compendium of international methods of analysis of wines and musts', published in 2018

by the International Organization of Vine and Wine (OIV): harvest, 2015 (2016); ethanol (% v/v), 11.47 (11.35); pH, 3.22 (3.16); titratable acidity (g/L of sulphuric acid), 4.40 (4.60); volatile acidity (g/L of sulphuric acid), 0.26 (0.45); malic acid content (g/L), <2.0 (< 2.0); free SO<sub>2</sub> (mg/L), < 9 (~4) and total SO<sub>2</sub> (mg/L), 5 (not measurable). After opening, the wine samples were stored under N<sub>2</sub> atmosphere.

## 2.2. Model wine solution

One litre of model wine solution consisting of 12% (v/v) ethanol and tartaric acid (8 g/L) was prepared and its pH was adjusted to 3.5 with 10 M NaOH. To guarantee air saturation, samples were stirred for 1 h before carrying out the experiment.

## 2.3. Measurement of Fe(II) chelating activity

First, the chelating activity of CHI-2 was determined in model wine (pH 3.5) at room temperature using the ferrozine competition assay (Stookey, 1970) with modifications. Briefly, 0.1 mL of CHI-2 in suspension at different concentrations (0–10 g/L) was mixed with 50 µL of ferrozine solution (0.7–2 mM) in 1.5 mL Eppendorf tubes. Following stirring of the samples for 10 min in darkness, 0.1 mL of Fe(II), as ferrous sulfate, (100 µM) was added and agitation was maintained for 48 h. Following centrifugation (2320 g) of the samples for 5 min, 0.2 mL of supernatant was transferred into 96-well microplates and the absorbance was determined at 562 nm using a microplate reader (Tecan Infinite, Männedorf, Switzerland). Plotting absorbance inhibition versus chitosan concentration allowed IC<sub>50</sub> values to be determined, defined as the effective chitosan (or ferrozine) concentration required to chelate 50% of iron(II). Calibration curves (from triplicate

measurements) were established in model wine at pH 3.5 by plotting absorbance versus ferrozine concentration (0.25–3 mM) at a given Fe(II) concentration (0.1–0.5 mM) using the same incubation protocol.

Second, the unchelated iron content of real wine samples spiked with 100  $\mu\text{M}$  Fe(II) alone or in the presence of CHI-2 (0.5 and 2 g/L) was also determined by means of flame atomic absorption according to the relevant OIV method (see above). Briefly, samples were saturated with air and aliquots (20 mL) were placed into 50-mL Falcon tubes sealed with stoppers and continuously agitated for 48 h at 20 °C in darkness. Afterwards, samples were centrifugated (45 g) and filtered prior to injection for iron analysis. The instrument was an Agilent 240FS AA spectrophotometer, with a deuterium lamp for background radiation correction, a hollow cathode lamp at 248.3 nm, and the air–acetylene flame. Calibration curves were plotted using standard iron diluted with deionized water. All analyses were performed in triplicate.

## 2.4. Irradiation and sample analysis

### 2.4.1. Wine sample preparation

An additional set of iron-spiked wine samples containing CHI-2 (0.5 and 2 g/L) or  $\text{SO}_2$ , as potassium metabisulfite, (50 mg/L) were prepared and stored as outlined for flame atomic absorption studies. Samples were placed at 20 °C in a temperature controlled chamber for 1–6 days at a distance of 5 cm from two cool daylight fluorescent lamps (Sylvania T8 Luxline Plus 36W 840) producing a light at 300–580 nm wavelength and an average intensity of 2000 lux. The light intensity was measured using a 51000 series digital lux meter (Yogokawa, Lyon, France). All samples were shaken for 2 min four times/day throughout. All experiments were performed at least in triplicate.

#### 2.4.2. HPLC-DAD analysis of acetaldehyde

At the end of the irradiation period the samples were analyzed for their content in acetaldehyde using a Merck Hitachi HPLC system consisting of an Elite LaChrom L-7000 interface module with a diode array detector (DAD) (L-7455) and a EZchrom workstation for data processing. The UV spectra were recorded in the range 220–400 nm. With the aim to detect exclusively the free fraction of aldehydes which take part in oxidation process, no acid hydrolysis of samples was carried out. Samples (800  $\mu\text{L}$ ) were incubated with 200  $\mu\text{L}$  of a DNPH solution (10 mM in 2.5 M HCl) for 1 h at 45° C in darkness. After cooling at room temperature separation of the DNPH adducts was achieved on a Nucleodur C18 Htec column (Macherey-Nagel, Düren, Germany; 250  $\times$  4.6 mm; 5  $\mu\text{m}$ ) with a flow rate of 0.8 mL/min. Solvent A was acetonitrile; solvent B was water containing 0.05% (v/v) solution of phosphoric acid (pH 2.7). The elution program was the following: 0 min, 40% A, 8 min, 85% A, 9 min, 40% A, 13 min, 40% A, and injection volume was 20  $\mu\text{L}$ . The identification of the observed derivatives was based on their retention time compared with those of standards tested at 360 nm as well as their spectral characteristics. Quantification was based on peak area.

#### 2.5. Oxygen radical absorbance capacity (ORAC) assay

The assay was performed in microplates as previously described (Kandouli et al., 2017). Briefly, a fluorescein stock solution (821  $\mu\text{M}$ ) was prepared in PBS and stored at 4 °C. Prior to use, the following solutions in  $\text{KH}_2\text{PO}_4$  buffer (0.1 M, pH 7.4) were prepared: fluorescein stock solution rediluted as to reach 82.1 nM, and AAPH (153 mM). Test samples, Trolox calibration solution or the blank (25  $\mu\text{L}$ /well) were added to the wells of a 96-well plate, diluted with fluorescein solution (150  $\mu\text{L}$ /well) and incubated for 10 min at 37

°C. AAPH solution (25  $\mu\text{L}$ /well, 19.12 mM, final concentration) was then added and the fluorescence intensity (excitation at 485 nm, emission at 530 nm) was monitored every 2 min for 70 min with a microplate reader. The ORAC value was calculated using the net area-under-curve and expressed as  $\mu\text{mol Trolox/ mL}$ .

## 2.6. Preparation of solutions and suspensions for EPR spin trapping analysis

Samples to be scanned by EPR were aspirated into 50  $\mu\text{L}$  glass capillary tubes (Hirschmann Lab., Eberstadt, Germany), as to fill them completely, and sealed with Critoseal (McCormick Scientific, St Louis, MO) at lower (nucleophilic addition and Fenton reaction with 4-MeC) or both ends (remaining studies).

### 2.6.1. Solutions for *in situ* photolysis and Fenton reaction in model wine and calculation of rate constants

Hydrogen peroxide (3% v/v) was used as photolytic precursor of  $\text{HO}\bullet$ . Solutions of chitosan (0.1–2 g/L) dissolved in water containing 0.5% (v/v) acetic acid (pH 3.18) and DMPO (3.33 mM, final) were continuously illuminated using a 1000 W xenon-mercury UV–Vis light source (Oriel, Newport Corp., Irvine, CA) guided within the EPR cavity through an optical glass fiber. The corresponding blank spectra were subtracted from experimental spectra before data processing.

The apparent second-order rate constant  $k_{\text{CHI}}$  for the reaction of  $\text{HO}\bullet$  with chitosan was calculated using the equation:

$$I_0/I = 1 + [(k_{\text{CHI}}/(k_{\text{DMPO}} \times C_{\text{DMPO}}) \times C_{\text{CHI}}]$$

where  $I_0$  and  $I$  is the intensity of the EPR signal recorded in the control and in presence of chitosan, respectively,  $C_{\text{DMPO}}$  and  $C_{\text{CHI}}$  are the concentrations of DMPO and chitosan, respectively, and  $k_{\text{DMPO}}$  is the second-order rate constant for the trapping of  $\text{HO}\bullet$  on DMPO. The slope of the regression plot of  $I_0/I$  against  $C_{\text{CHI}}$  for a constant value of  $C_{\text{DMPO}}$  was used to estimate  $k_{\text{CHI}}$  (Finkelstein, Rosen & Rauckman, 1980):

$$k_{\text{CHI}} = \text{slope} \times C_{\text{DMPO}} \times k_{\text{DMPO}}$$

assuming that  $k_{\text{DMPO}} = 3.4 \times 10^9 \text{ M}^{-1} \cdot \text{s}^{-1}$  using the above conditions and photolytic system (Finkelstein et al., 1980).

To estimate the effect of hydrogen peroxide and iron(II) on Fenton-driven 4-POBN spin adduct formation  $\text{H}_2\text{O}_2$  (0.25–25  $\mu\text{g}/\text{mL}$ ) was added to a freshly prepared solution of the nitron (15 mM) and Fe(II) (0.1 or 0.2 mM) in model wine. EPR spectra were acquired 130 s or 10 min after addition of  $\text{H}_2\text{O}_2$ .

### 2.6.2. Suspensions for nucleophilic addition assays

A suspension of tested chitosan (0.5–2 g/L) in water containing a wine relevant concentration of Fe(III), as  $\text{FeCl}_3$ , of 30 mg/L and Cu(II), as  $\text{CuSO}_4$ , of 12.5 mg/L was stirred for 1 h at room temperature to allow for metal complexation by chitosan. EPR spectra were recorded 1 min following addition of aqueous DEPMPO (55 mM) to the suspension.

### 2.6.3. Suspensions for Fenton reaction assays and incubations

All experiments described below (incubations and EPR spectrometry) were conducted at 20–22 °C in darkness.

To assess the effect of CHI-2 (0.5 or 2 g/L) or SO<sub>2</sub> (50 mg/L) on 4-POBN adduct formation the tested inhibitor was pre-incubated with 100 μM Fe(II) for 48 h in model wine. Following pre-incubation of suspensions/solutions were added the nitron (15 mM) and H<sub>2</sub>O<sub>2</sub> (2.5 μg/mL) dissolved in model wine. EPR spectra were then sequentially recorded up to 1 h following addition of H<sub>2</sub>O<sub>2</sub>. In some experiments 4-MeC (1 mM) was also added after pre-incubation.

To extend the above experiments to wine oxidation under winemaking conditions the incubations were prolonged up to 3 or 6 days in model and real wine, respectively. A 48-h pre-incubation with 100 μM of Fe(II) and varying concentrations of the tested inhibitor (i.e., chitosan, SO<sub>2</sub> or ferrozine) was first applied. Then 4-POBN (15 mM) alone (real wine) or mixed with 4-MeC (1 mM; model wine) were added and the EPR signal intensity was followed over time. In experiments performed in real wine samples were gently decanted by centrifugation at 25 g for 5 min before adding the nitron in the clear supernatant.

Throughout incubation the solutions/suspensions were stored in capped Eppendorf tubes with a ~10 times air volume above and stirred at 5–10 rpm with a Stuart SB3 rotator (Cole-Parmer, Vernon Hills, IL).

## 2.7. Acquisition of EPR spectra and apparatus

EPR signals were obtained with a Bruker ESP 300 spectrometer (Karlsruhe, Germany) operating at X-band (9.79 GHz) with 100 kHz modulation frequency and a microwave power of 10 mW. Typical settings in DMPO and 4-POBN (DEPMPO) spin trapping were: modulation amplitude, 0.625 (0.279) G; time constant, 81.92 (40.96) ms; gain, 1 × 10<sup>5</sup> (1.25 × 10<sup>5</sup>); sweep width, 60 (140) G; sweep time/scan, 41.94 (41.94) s; number of accumulated scans, 10 (1). To determine *g*-factors the magnetic field strength and

microwave frequency were measured with a Bruker ER 035M NMR gaussmeter and a Hewlett Packard 5350B frequency counter, respectively. Spin adduct intensities were determined by double integration of simulated spectra using WinSim software (Duling, 1994). Area-under-curve of spin adduct variations were obtained using Prism software (GraphPad Software, San Diego, CA).

### 2.8. Statistical analysis

Data are given as mean  $\pm$  SEM for the indicated number of independent experiments. Evaluation of statistical significance was conducted by one-way analysis of variance (ANOVA) followed, if significant ( $p < 0.05$ ), by a posteriori Duncan test. Differences between groups were considered significant when  $p < 0.05$ .

## 3. Results and discussion

Owing to its insolubility at wine pH and known metal chelation property, suspensions of chitosan were stirred for 2 days in darkness with 100  $\mu\text{M}$  (5.5 mg/L) Fe(II), a typical concentration found in white wine, to ensure maximum metal chelation before oxidation under wine conditions was induced. Under these pre-incubation conditions 500  $\mu\text{M}$  ferrozine were found to chelate 142  $\mu\text{M}$  of Fe(II) in model wine at pH 3.5, while increasing the pH to 4.5 resulted in a 30% increase of the chelating power, in agreement with previous observations (Stookey, 1970).

### 3.1. EPR evidence that chitosan slows free radical formation during wine oxidation

A general method to follow 1-HER formation in oenology as an intermediate in non-enzymatic wine oxidation (Fig. 1) is to apply EPR spin trapping using the linear aryl nitron 4-POBN as the spin trap (Elias et al., 2009a, 2009b; Nikolantonaki et al. 2019). Thus, in 4-POBN (15 mM)-containing model wine (12% v/v ethanol, 8 g/L tartaric acid, pH 3.5) challenged by HO• radicals formed via a Fenton reaction, the strong six-lines spectrum of 4-POBN-1-HER spin adduct was detected, with hyperfine splittings:  $a_N = 15.62$  G,  $a_H = 2.55$  G,  $a_{13-C} = 5.22$  G, and  $g = 2.0054$  in good agreement with previous data, including the coupling value of the  $^{13}\text{C}$  satellite lines (Halpern, Yu, Barth, Peric & Rosen, 1995; Nakao & Augusto, 1998; Pou et al., 1994). In the same system removal of ethanol allowed transient detection of the 4-POBN/hydroxyl radical adduct (4-POBN-OH) as a sextet with slightly different EPR parameters:  $a_N = 14.99$  G,  $a_H = 1.65$  G, and  $g = 2.0057$ , consistent with early data (Pou et al., 1994). The fact that 1-HER, and not the primarily formed HO• (Fig. 1), is the major species trapped in 4-POBN spin trapping studies on alcoholic beverages mainly relies on: (i) the very low stability of 4-POBN-OH versus 4-POBN-1-HER (Halpern et al., 1995; Pou et al., 1994), and (ii) the large excess of ethanol (molar range) with respect to the nitron (millimolar range) in the system to compete with HO•. Indeed, detection of nitron/HO• adducts in oxidizing wine required a molar concentration of the trap (Elias et al., 2009a).

As depicted in Fig. 1 endogenous wine's phenolics can be considered suitable Fe(II)/Fe(III) redox recyclers to sustain the Fenton reaction involved in wine oxidation (Elias et al., 2009a; Elias & Waterhouse, 2010). When the model wine system above had 1 mM of 4-MeC added (taken as a model for wine's catechols), a wine's typical concentration with respect to total phenolics (Kreitman, et al., 2013b), 4-POBN-1-HER adducts developed over 3 days at ambient temperature and in darkness, provided that

incubating samples were always well aerated. Given the known high stability and resistance to redox-active agents of 4-POBN-1-HER adducts (Halpern et al., 1995) a sensitive EPR acquisition method was applied here, where accumulating signals in ~7-min blocks allowed detection of weak signal intensities since 1 h in control samples (Fig. 3A). Both chitosans added in suspension up to 2 g/L significantly inhibited oxidative formation of 4-POBN-1-HER with similar profiles (but no clear dose-dependence), CHI-2 being the most effective after 48 h of action. A very significant inhibitory effect of the best compound, CHI-2, added at 1 or 2 g/L was also seen when incubations were carried out in sulphite-free Chardonnay wine for up to 6 days at ambient temperature, again with no significant dose effect except in the early oxidation phase (Fig. 3B).

In order to address the mechanisms by which chitosans protect synthetic and real wine against free radical mediated ethanol oxidation, i.e., by delaying the formation of 1-HER radical intermediate, incubations in both matrices were carried out in the presence of SO<sub>2</sub> at a winemaking dose (50 mg/L), or the strong iron(II) chelator ferrozine. By interacting with two main components of the Fenton system (Fig. 1), SO<sub>2</sub> and ferrozine can inhibit 1-HER formation by removing H<sub>2</sub>O<sub>2</sub> or forming iron complexes with no catalytic power, respectively (Elias et al., 2009b; Elias & Waterhouse, 2010; Kreitman et al. 2013b). The strong decreases in 4-POBN-1-HER formation seen with both types of treatments seem to confirm the pertinence of these two mechanisms (Fig. 3). Thus, spin adduct formation re-increased in SO<sub>2</sub> added samples after 48 h incubation, possibly because decreased levels of free SO<sub>2</sub> (i.e., the scavenging-active SO<sub>2</sub> fraction not linked to acetaldehyde and not already oxidized to sulfate) could no more efficiently eliminate the continuous H<sub>2</sub>O<sub>2</sub> formation in the system.

EPR signals from all samples pre-treated with high ferrozine (500 µM) exhibited the lowest intensities throughout the incubation time frame (Fig. 3). This is consistent with the

results of the Fe(II) activity assay above suggesting that practically all of the 100  $\mu\text{M}$  iron(II) added should have been complexed by ferrozine into a Fenton-inactive species. Moreover, from the  $\text{IC}_{50}$  values obtained by the ferrozine assay in model wine it was found that 168  $\mu\text{M}$  ferrozine and 2.4 g/L CHI-2 exhibited similar chelating effects toward 100  $\mu\text{M}$  of Fe(II). This could explain the similarity of 4-POBN-1-HER inhibition profiles between samples supplied with 150  $\mu\text{M}$  ferrozine and those with added CHI-2, but not CHI-1 (Fig. 3A).

The extent to which pre-treating the real wine with CHI-2 had reduced the amount of catalytic Fe(II) before the spin trapping reaction shown in Fig. 3B started, was quantified by flame atomic absorption. The endogenous concentration of Fe in the wine was only of  $6.8 \pm 0.1 \mu\text{M}$  (both vintages combined). Following addition of 100  $\mu\text{M}$  Fe(II) and incubation for 2 days in darkness,  $98.9 \pm 1.1 \mu\text{M}$  of iron was detected, with a small loss consequent to, e.g., adsorption onto the labware or wine proteins, or chelation by tartaric or citric acids. In the presence of CHI-2 at 0.5 and 2 g/L, the free iron content of the wine samples was significantly decreased to  $48.5 \pm 0.4$  and  $31.2 \pm 0.8 \mu\text{M}$ , respectively.

It is therefore possible that part of the effect of chitosans found in the above EPR experiments may be due to Fe(II) chelation properties. Chelation capacity of chitosan in oenology has already been reported (Bornet & Teissedre, 2008; Chinnici et al., 2014; Colangelo et al., 2018). Since for these compounds metal removal is based on the formation of a complex involving amine or hydroxyl groups (Fig. 1), chelation capacity increases with increasing degree of deacetylation and decreasing molecular weight as a consequence of greater availability of amino groups toward metal ions (Bornet & Teissedre, 2008). These structural features may explain the lower effectiveness of CHI-1 versus CHI-2 (Fig. 3A). Furthermore, chitosan can adsorb polyphenols into its matrix, decreasing their level in wine (Chinnici et al., 2014; Spagna et al., 1996). Hence, such a

decrease in the 4-MeC (model wine) or oxidizable polyphenols (real wine) contents would indirectly inhibit spin adduct formation by lowering  $H_2O_2$  levels.

### 3.2. Mechanistic understanding of the inhibitory effect of chitosan

#### 3.2.1. Quantification of $H_2O_2$ levels occurring during wine oxidation

In the above experiments the relative EPR intensities were found to be similar over the incubation time frame regardless experiments were performed in 4-MeC-supplemented model or real wine (Fig. 3). To estimate the  $H_2O_2$  concentrations implicated, a Fenton assay was run in unsupplemented model wine by measuring 4-POBN-1-HER levels, obtained using an identical temperature and acquisition protocol, as a function of Fe(II) and  $H_2O_2$  constituents. As seen in Fig. 4, spin adduct concentration, which increased with any of these two constituents, was more dramatically affected upon doubling iron(II) content than when  $H_2O_2$  concentration was increased 10 times. This substantiates the above and previous findings (Bornet & Teissedre, 2008; Elias et al., 2009b; Kreitman et al., 2013b) that decreasing metal ion content in wine may be a more sustainable strategy against oxidation than temporarily scavenging  $H_2O_2$  by adding  $SO_2$ . Furthermore, in completely filled and stopped capillaries, 4-POBN-1-HER intensities only moderately augmented 10 min versus ~2 min after triggering the Fenton reaction, and consequently the generation/detection system run here can be considered as a controlled one.

As seen in Fig. 3, accumulation of long-lived 1-POBN-1-HER adducts resulted in average EPR intensities peaking at ~2.5 relative units in the controls when 100  $\mu$ M Fe(II) was used to start oxidation. According to the results of Fig. 4 where  $H_2O_2$  was added at once in the system, this suggests that the total  $H_2O_2$  concentration decomposed by the Fenton reaction over 3–6 days under wine oxidation conditions was very low, ranging

0.25–2.5  $\mu\text{g}/\text{mL}$  (7–75  $\mu\text{M}$ ), as visualized by the dashed line in Fig. 4. Fenton generators commonly used in wine oxidation spin trapping studies involve similar Fe(II) concentrations but at least fourfold higher  $\text{H}_2\text{O}_2$  concentrations (Elias et al., 2009a; Nikolantonaki et al., 2019). Obviously, the EPR spin trapping technique applied here underestimates  $\text{H}_2\text{O}_2$  levels produced in wine oxidation because a variety of scavenging mechanisms are operating, e.g., reactions with  $\text{SO}_2$ . Thus in a set of red wines oxidized in air at  $40^\circ\text{C}$  using 100  $\mu\text{M}$  Fe(II), a rate of  $\text{H}_2\text{O}_2$  formation of  $\sim 14 \mu\text{M}/30 \text{ min}$  was reported (Héritier, Bach, Schönberger, Gaillard, Ducruet & Segura, 2016).

### 3.2.2. Effect on Fenton-derived 1-HER

Having defined the combination of 100  $\mu\text{M}$  Fe(II) + 2.5  $\mu\text{g}/\text{mL}$   $\text{H}_2\text{O}_2$  (74  $\mu\text{M}$ ) as a wine-like Fenton system to model incubations of Fig. 3A, it was applied in model wine  $\pm$  4-MeC (1 mM), alone or in the presence of inhibitors, and the effects on 4-POBN-1-HER formation were monitored for up to 1 h. In unsupplemented medium EPR signals, which expectedly increased along with the continuous formation of  $\text{HO}\bullet$  radicals, showed a 2.5–3.5 amplification in the presence of 4-MeC (Fig. 5A). A similar effect has been reported by Elias and Waterhouse (2010) who suggested that the recycling of Fe(III) to Fe(II) by 4-MeC may increase adventitiously the amount of 1-HER available for spin trapping (Fig. 1). The control EPR signals in Fig. 5A were decreased up to 89% (unsupplemented) or 95% (with 4-MeC) in samples pre-incubated with CHI-2 suspensions (0.5 or 2 g/L) for 2 days, with no clear dose-response effect. In these experiments background 4-POBN-1-HER adducts were detected in  $\text{SO}_2$  added samples up to 30 min.

### 3.2.3. Effect on photochemically generated hydroxyl radicals

Having investigated the iron(II) chelating property of chitosans as a key step of the inhibition of HO•-mediated wine oxidation, additional spin trapping experiments were carried out in attempt to delineate the specific HO• scavenging behaviour of these compounds. Previous EPR investigations of the antioxidant properties of chitosan have generally focused on hydrosoluble derivatives and standard assays, including Fenton reaction-based tests on HO• scavenging (see, e.g., (Park, Je & Kim, 2003)) for which there is clear interference with Fe(II) chelation property. Here, an iron independent method for producing HO• spin adducts was used, where in situ photolysis of 3% H<sub>2</sub>O<sub>2</sub> in the presence of the cyclic nitron DMPO (ca. 3 mM) in 0.5% acetic acid solution (pH 3.2) afforded the known DMPO/hydroxyl radical adduct (DMPO-OH), giving a characteristic 1:2:2:1 EPR quartet with  $a_N = a_H = 14.95$  G and  $g = 2.0053$  (Fig. 2b).

Both chitosans, soluble in the medium up to 2 g/L, dose-dependently inhibited the formation of DMPO-OH. Using the kinetic analysis of (Finkelstein et al., 1980) plots of  $I_0/I$  against concentration were obtained (see Methods), exhibiting satisfactory linear fits (Fig. 5B). Assuming an average molecular weight of 120 and 20 kDa for CHI-1 and CHI-2, respectively, second-order rate constants for the reaction of HO• were calculated as  $7 \times 10^{12}$  and  $10^{12}$  M<sup>-1</sup>.s<sup>-1</sup> for CHI-1 and CHI-2, respectively. Such high values, reflecting diffusion-controlled processes, have been reported for many macromolecules, including proteins (Bailey et al., 2014). Using pulse radiolysis, a technique more specific for determining HO• rate constants, a value of  $6.3 \times 10^8$  M<sup>-1</sup>.s<sup>-1</sup> has been reported for deacetylated chitosan from a crustacean, krill (*Euphausia superba*) at pH 3 (Ulanski & von Sonntag, 2000).

As displayed in Fig. 1, molecular mechanisms for HO• scavenging by chitosan backbone can involve either free amine groups and/or their ammonium derivatives, or typical H-abstraction reactions along the polysaccharide unit (Xie, Xu & Liu, 2001). Moreover, earlier EPR and pulse radiolysis studies have revealed a low selectivity for H-

abstraction onto the chitosan unit, i.e., these compounds would behave as if a single preferred site was submitted to HO• attack (Ulanski & von Sonntag, 2000). This could explain the linear variations of Fig. 5B, with intercepts of 1.1 and 1.5 for CHI-1 and CHI-2, respectively, close to the theoretical value of 1 in the kinetic model of (Finkelstein et al., 1980).

In another approach to discriminate between iron chelation and free radical scavenging in the inhibitions seen in Fig. 3 the ORAC-fluorescein values were calculated for tested wines. This method, which measures the scavenging efficacy against a peroxy radical formed by thermal scission of an azo initiator, AAPH, has been widely applied to assess the antioxidant capacity of wine (Sánchez-Moreno, Cao, Ou, & Prior, 2003; Stockham et al., 2013), a high ORAC showing a better antioxidative power. In this study the ORAC found for experimental wine, typical of Chardonnay wines (Sánchez-Moreno et al., 2003; Stockham et al., 2013), is yet twice as low as that for 4-MeC containing synthetic wine (Table 1). If radical scavenging was the dominant mechanism this would lead in principle to lower levels of 4-POBN-1-HER in the model vs. the real wine in the incubation controls with no added iron chelator. To estimate these levels the area-under-curves (AUC) of Fig. 3A were calculated and the expected [2 (real wine):1 (model wine)] ratio was obtained in control experiments only during the first incubation day, consistent with differences in ORACs (Table 1). Therefore, further decrease of this ratio found up to day 3 may suggest a shift from dominant radical scavenging to other inhibitory mechanisms, e.g., delayed Fe(II) chelation by 4-MeC or other wine phenolics. In samples incubated with CHI-2 (2 g/L) the same AUC analysis, yielding expected lower values, also demonstrated a nearly constant 2:1 ratio. This suggests that, once iron had been removed by the 2-days pre-treatment, it is the antioxidant property of chitosan that could have caused the lower spin adduct levels observed. It is worth mentioning, however, that good correlations

between ORAC assay and EPR spin trapping have been only reported for peroxy, but not hydroxyl radicals (Kameya, Watanabe, Takano-Ishikawa & Todoriki, 2014).

#### 3.2.4. Effect on cupric and ferric ions

Adding copper, as Cu(II), during the winemaking process is a common practice, in particular to decrease the levels of sulfur containing compounds responsible for off-flavors before bottling of white wines. Since cupric ions can catalyze H<sub>2</sub>O<sub>2</sub> degradation by a Fenton-like mechanism (Hanna & Mason, 1992), they would potentiate the effect of Fe(III) in wine oxidation (Danilewicz, 2003). In wine studies, however, use of spin trapping is complicated because Cu(II) often induce degradation of nitrones into unwanted nitroxides and/or lead to paradoxical 1-HER formation profiles (Elias et al., 2009b).

In this study EPR has been used to assess indirectly the effect of chitosans on iron and copper at wine-like concentrations, by measuring the impact on nucleophilic induced spin adduct formation. Thus, by forming a transient complex at the nitronyl oxygen of spin traps such as DMPO or its phosphorylated analog, DEPMPO, Fe(III) or Cu(II) catalyze the nucleophilic addition of water to form the corresponding hydroxyl radical adduct, and this reaction is inhibited by Fe(III) (Culcasi et al., 2006a) and Cu(II) (Hanna & Mason, 1992) chelators. When an aqueous solution of DEPMPO (55 mM), a chiral molecule (Fig. 2), was added to a mixture of wine-like 30 mg/L Fe(III) and 12.5 mg/L Cu(II), a major 8-lines EPR spectrum was observed (Fig. 2c). A satisfactory fit was obtained assuming a mixture of EPR-distinguishable diastereoisomeric DEPMPO/hydroxyl radical adducts (DEPMPO-OH) with the following parameters (couplings in G): *cis*-DEPMPO-OH ( $a_N = 14.05$ ,  $a_P = 47.25$ ,  $a_H = 14.13$ ), and *trans*-DEPMPO-OH ( $a_N = 14.05$ ,  $a_P = 47.22$ , and  $a_H = 12.73$ ), and  $g = 2.0057$ . A minor carbon-centered DEPMPO adduct was also detected ( $a_N = 14.32$  G,  $a_P = 45.91$  G,  $a_H = 21.36$  G), possibly due to some degradation of the trap by Cu(II), and

accounting for 24% of the total signal. The *cis:trans* ratio in Fig. 2c was of 36:64, consistent with a HO• scavenging-unrelated, nucleophilic addition mechanism (Culcasi et al., 2006b). When metal added solutions were stirred for 1 h at ambient temperature in the presence of varying amounts of chitosan, further addition of DEPMPO to the suspensions led to dose dependently decreased DEPMPO-OH levels, by 73–92%, with no differences between chitosans (Fig. 5C). Altogether these results demonstrated sequestration of Fe(III) / Cu(II) as another facet of the inhibitory action of chitosan in wine oxidation. Accordingly, chitosan has been shown to adsorb iron from wines spiked with ferric ions (Bornet & Teissedre, 2008).

### 3.2.5. Effect on photooxidation-induced acetaldehyde formation

To substantiate the effect of CHI-2 seen in Fig. 3B the production of acetaldehyde was monitored by HPLC-DAD in experimental wine spiked with 100 µM Fe(II) and irradiated with fluorescent light (300–580 nm) for up to 6 days at ambient temperature. Long term exposure to sunlight or fluorescent tubes has been shown to contribute to the development of browning and the formation of off-odors in white wine. In wine conditions (pH and metals) a main proportion of carboxylic acids in wine, such as tartaric and lactic acids, exist as Fe(III) carboxylate complexes, the irradiation of which leads to a range of carbonyls, including acetaldehyde. This in turn will release free Fe(II), providing an additional source of catalytic iron to fuel the Fenton system, a forced oxidation mechanism termed as 'photo-Fenton' (Grant-Preece et al., 2017).

At opening, acetaldehyde concentration of experimental SO<sub>2</sub> free wine was  $7.6 \pm 0.7$  mg/L (mean value from both vintages), falling within the lowest acetaldehyde concentrations reported in just finished, sulphited dry white wines (Jackowetz & de Orduña, 2013). Following initial production by yeasts during fermentation acetaldehyde

can be further synthesized from ethanol through Fenton oxidative degradation (Fig. 1). Here this second source of acetaldehyde is likely poorly active since when the wine was stored for 2 days in darkness with a 1.5 times air volume in the headspace, a non significant increase to  $9.1 \pm 0.2$  mg/L was found, possibly because catalytic iron present in the wine was only  $\sim 0.4$  mg/L. Wine samples added 5.5 mg/L Fe(II) and incubated in darkness for 2 days, which retained 5.4 mg/L iron after filtration, showed, however, non significantly increased acetaldehyde levels of  $10.8 \pm 0.4$  mg/L (Table 1). Under photo-Fenton conditions acetaldehyde in the controls increased significantly afterwards, doubling after 6 days irradiation. In wine samples spiked with 5.5 mg/L Fe(II) and having had their iron content lowered by 51% and 68% after 2 days in contact with CHI-2 at 0.5 and 2 g/L, respectively, this irradiation-induced elevation of acetaldehyde concentration was significantly inhibited, with decreases of 19% and 38%, respectively, at day 6 (Table 1). Being a strong binder for sulphur dioxide (Oliveira et al., 2011) free acetaldehyde expectedly exhibited the lowest concentrations in irradiated wine added SO<sub>2</sub> (50 mg/L). However, after 6 days of light exposure, once complete oxidation and/or binding of SO<sub>2</sub> was reached, acetaldehyde production in those samples was not statistically different from that in samples containing 2 g/L CHI-2 (Table 1) and therefore the acetaldehyde inhibition pattern in CHI-2 added wine paralleled that seen for 1-HER formation in Fig. 3B.

#### 4. Conclusion

The results of this study strengthen current interest in using chitosan as a substitute for and/or complement to lower sulphur dioxide and sulphites in winemaking. By monitoring the formation of spin trapped 1-HER, a pivotal intermediate of wine oxidation, EPR analysis sought to establish a chronology of chitosan antioxidant action under wine

relevant doses, application and aging conditions. It was found that once the catalytic activity of the metal pool in wine, especially Fe(II)/Fe(III), has been partly deactivated by chelation, direct scavenging of oxidizing species such as HO• continuing to form at slow rates may represent a significant inhibitory mechanism of chitosan. In this regard, the well documented metal ions-sensitive depolymerization of chitosan by H<sub>2</sub>O<sub>2</sub> (Chang, Tai & Cheng, 2001) could be an additional protective effect against wine oxidation as depicted in Fig. 1. Studies are in progress to verify, using specific tests, if a related free radical-independent mechanism could participate in the effects seen in the present study.

Of note, the significant impact of chitosans against free radical formation seen here was obtained as the compounds were directly added in suspension in the finished wine. This will encourage designing future spin trapping studies using EPR techniques specific for large heterogenous samples to follow in situ oxidation of white musts during the alcoholic fermentation.

### **Acknowledgments**

The authors thank G. Excoffier at Spectropole (Aix Marseille Université) for his expert assistance in atomic flame absorption analyses and P. Bernasconi for maintenance of the EPR device.

### **Conflict of interest**

The authors declare that there are no conflicts of interest.

### **Funding**

This study was supported by grants from CNRS and Aix Marseille University. Part of this study (DEPMPO synthesis and purification) was supported by fundings of the Agence Nationale de la Recherche (ANR JCJC MitoDiaPM – N° ANR-17-CE34-0006-01).

ACM acknowledges the Marco Polo program from University of Bologna for funding the research stay at the ICR, Marseille.

## References

- Bailey, D. M., Lundby, C., Berg, R. M. G., Taudorf, S., Rahmouni, H., Gutowski, M., Mulholland, C. W., Sullivan, J. L., Swenson, E. R., McEneny, J., Young, I. S., Pedersen, B. K., Moller, K., Pietri, S., & Culcasi, M. (2014). On the antioxidant properties of erythropoietin and its association with the oxidative-nitrosative stress response to hypoxia in humans. *Acta Physiologica*, *212*, 175–187.
- Bornet, A., & Teissedre, P. L. (2008). Chitosan, chitin-glucan and chitin effects on minerals (iron, lead, cadmium) and organic (ochratoxin A) contaminants in wines. *European Food Research and Technology*, *226*, 681–689.
- Castro-Marín, A., Buglia, A. G., Riponi, C., & Chinnici, F. (2018). Volatile and fixed composition of sulphite-free white wines obtained after fermentation in the presence of chitosan. *LWT - Food Science and Technology*, *93*, 174–180.
- Chang, K. L. B., Tai, M. C., & Cheng, F. H. (2001). Kinetics and products of the degradation of chitosan by hydrogen peroxide. *Journal of Agricultural and Food Chemistry*, *49*, 4845–4851.
- Chinnici, F., Natali, N., & Riponi, C. (2014). Efficacy of chitosan in inhibiting the oxidation

of (+)-catechin in white wine model solutions. *Journal of Agricultural and Food Chemistry*, 62, 9868–9875.

Colangelo, D., Torchio, F., De Faveri, D. M., & Lambri, M. (2018). The use of chitosan as alternative to bentonite for wine fining: Effects on heat-stability, proteins, organic acids, colour, and volatile compounds in an aromatic white wine. *Food Chemistry*, 264, 301–309.

Culcasi, M., Rockenbauer, A., Mercier, A., Clément, J. L., & Pietri, S. (2006a). The line asymmetry of electron spin resonance spectra as a tool to determine the *cis:trans* ratio for spin-trapping adducts of chiral pyrrolines *N*-oxides: The mechanism of formation of hydroxyl radical adducts of EMPO, DEPMPO, and DIPPMPPO in the ischemic-reperfused rat liver. *Free Radical Biology and Medicine*, 40, 1524–1538.

Culcasi, M., Muller, A., Mercier, A., Clément, J.-L., Payet, O., Rockenbauer, A., Marchand, V., & Pietri, S. (2006b). Early specific free radical-related cytotoxicity of gas phase cigarette smoke and its paradoxical temporary inhibition by tar: An electron paramagnetic resonance study with the spin trap DEPMPO. *Chemico-Biological Interactions*, 164, 215–231.

Danilewicz, J. C. (2003). Review of reaction mechanisms of oxygen and proposed intermediate reduction products in wine: central role of iron and copper. *American Journal of Enology and Viticulture*, 54, 73–85.

Duling, D. R. (1994). Simulation of multiple isotropic spin-trap EPR spectra. *Journal of Magnetic Resonance, Series B*, 104, 105–110.

Elias, R. J., Andersen, M. L., Skibsted, L. H., & Waterhouse, A. L. (2009a). Identification of free radical intermediates in oxidized wine using electron paramagnetic resonance spin trapping. *Journal of Agricultural and Food Chemistry*, 57, 4359–4365.

- Elias, R. J., Andersen, M. L., Skibsted, L. H., & Waterhouse, A. L. (2009b). Key factors affecting radical formation in wine studied by spin trapping and EPR spectroscopy. *American Journal of Enology and Viticulture*, *60*, 471–476.
- Elias, R. J., & Waterhouse, A. L. (2010). Controlling the Fenton reaction in wine. *Journal of Agricultural and Food Chemistry*, *58*, 1699–1707.
- Filipe-Ribeiro, L., Cosme, F., & Nunes, F. M. (2018). Reducing the negative sensory impact of volatile phenols in red wine with different chitosans: Effect of structure on efficiency. *Food Chemistry*, *242*, 591–600.
- Finkelstein, E., Rosen, G. M., & Rauckman, E. J. (1980). Spin Trapping. Kinetics of the reaction of superoxide and hydroxyl radicals with nitrones. *Journal of the American Chemical Society*, *102*, 4994–4999.
- Grant-Preece, P., Barril, C., Schmidtke, L. M., & Clark, A. C. (2017). Impact of fluorescent lighting on the browning potential of model wine solutions containing organic acids and iron. *Journal of Agricultural and Food Chemistry*, *65*, 2383–2393.
- Halpern, H. J., Yu, C., Barth, E., Peric, M., & Rosen, G. M. (1995). In situ detection, by spin trapping, of hydroxyl radical markers produced from ionizing radiation in the tumor of a living mouse. *Proceedings of the National Academy of Sciences of the United States of America*, *92*, 796–800.
- Hanna, P. M., & Mason, R. P. (1992). Direct evidence for inhibition of free radical formation from Cu(I) and hydrogen peroxide by glutathione and other potential ligands using the EPR spin-trapping technique. *Archives of Biochemistry and Biophysics*, *295*, 205–213.
- Héritier, J., Bach, B., Schönenberger, P., Gaillard, V., Ducruet, J., & Segura, J. M. (2016). Quantification of the production of hydrogen peroxide H<sub>2</sub>O<sub>2</sub> during accelerated wine

oxidation. *Food Chemistry*, 211, 957–962.

Jackowetz, J. N., & de Orduña, R. M. (2013). Survey of SO<sub>2</sub> binding carbonyls in 237 red and white table wines. *Food Control*, 32, 687–692.

Kameya, H., Watanabe, J., Takano-Ishikawa, Y., & Todoriki, S. (2014). Comparison of scavenging capacities of vegetables by ORAC and EPR. *Food Chemistry*, 145, 866–873.

Kandouli, C., Cassien, M., Mercier, A., Delehedde, C., Ricquebourg, E., Stocker, P., Mekaouche, M., Leulmi, Z., Mechakra, A., Thétiot-Laurent, S., Culcasi, M., & Pietri, S. (2017). Antidiabetic, antioxidant and anti inflammatory properties of water and n-butanol soluble extracts from Saharian *Anvillea radiata* in high-fat-diet fed mice. *Journal of Ethnopharmacology*, 207, 251–267.

Kemp, B., Alexandre, H., Robillard, B., & Marchal, R. (2015). Effect of production phase on bottle-fermented sparkling wine quality. *Journal of Agricultural and Food Chemistry*, 63, 19–38.

Kreitman, G. Y., Laurie, V. F., & Elias, R. J. (2013a). Investigation of ethyl radical quenching by phenolics and thiols in model wine. *Journal of Agricultural and Food Chemistry*, 61, 685–692.

Kreitman, G. Y., Cantu, A., Waterhouse, A. L., & Elias, R. J. (2013b). Effect of metal chelators on the oxidative stability of model wine. *Journal of Agricultural and Food Chemistry*, 61, 1082–1087.

Nakao, L. S., & Augusto, O. (1998). Nucleic acid alkylation by free radical metabolites of ethanol. Formation of 8-(1-hydroxyethyl)guanine and 8-(2-hydroxyethyl)guanine Adducts. *Chemical Research in Toxicology*, 11, 888–894.

Nikolantonaki, M., Coelho, C., Noret, L., Zerbib, M., Vileno, B., Champion, D., & Gougeon,

- R. D. (2019). Measurement of white wines resistance against oxidation by electron paramagnetic resonance spectroscopy. *Food Chemistry*, 270, 156–161.
- Oliveira, C. M., Ferreira, A. C. S., De Freitas, V., & Silva, A. M. S. (2011). Oxidation mechanisms occurring in wines. *Food Research International*, 44, 1115–1126.
- Park, P. J., Je, J. Y., & Kim, S. K. (2003). Free radical scavenging activity of chitooligosaccharides by electron spin resonance spectrometry. *Journal of Agricultural and Food Chemistry*, 51, 4624–4627.
- Pou, S., Ramos, C. L., Gladwell, T., Renks, E., Centra, M., Young, D., Cohen, M. S., & Rosen, G. M. (1994). A kinetic approach to the selection of a sensitive spin trapping system for the detection of hydroxyl radical. *Analytical Biochemistry*, 217, 76–83.
- Sánchez-Moreno, C., Cao, G., Ou, B., & Prior, R. L. (2003). Anthocyanin and proanthocyanidin content in selected white and red wines. Oxygen radical absorbance capacity comparison with nontraditional wines obtained from highbush blueberry. *Journal of Agricultural and Food Chemistry*, 51, 4889–4896.
- Santos, M. C., Nunes, C., Saraiva, J. A., & Coimbra, M. A. (2012). Chemical and physical methodologies for the replacement/reduction of sulphur dioxide use during winemaking: Review of their potentialities and limitations. *European Food Research and Technology*, 234, 1–12.
- Spagna, G., Pifferi, P. G., Rangoni, C., Mattivi, F., Nicolini, G., & Palmonari, R. (1996). The stabilization of white wines by adsorption of phenolic compounds on chitin and chitosan. *Food Research International*, 29, 241–248.
- Stockham, K., Sheard, A., Paimin, R., Buddhadasa, S., Duong, S., Orbell, J. D., & Murdoch, T. (2013). Comparative studies on the antioxidant properties and polyphenolic content of wine from different growing regions and vintages, a pilot study

to investigate chemical markers for climate change. *Food Chemistry*, 140, 500–506.

Stookey, L. L. (1970). Ferrozine: A new spectrophotometric reagent for iron. *Analytical Chemistry*, 42, 779–781.

Ulanski, P., & von Sonntag, C. (2000). OH-Radical-induced chain scission of chitosan in the absence and presence of dioxygen. *Journal of the Chemical Society, Perkin Transactions 2*, 2, 2022–2028.

Vally, H., Misso, N. L. A., & Madan, V. (2009). Clinical effects of sulphite additives. *Clinical & Experimental Allergy*, 39, 1643–1651.

Waterhouse, A. L., & Laurie, V. F. (2006). Oxidation of wine phenolics: A critical evaluation and hypotheses. *American Journal of Enology and Viticulture*, 57, 306–313.

Xie, W., Xu, P., & Liu, Q. (2001). Antioxidant activity of water-soluble chitosan derivatives. *Bioorganic & Medicinal Chemistry Letters*, 11, 1699–1701.

Zhang, Q. A., Shen, Y., Fan, X. H., García Martín, J. F., Wang, X., & Song, Y. (2015). Free radical generation induced by ultrasound in red wine and model wine: an EPR spin-trapping study. *Ultrasonics Sonochemistry*, 27, 96–101.

Figure captions

**Fig. 1.** Free radical mediated formation of acetaldehyde from ethanol during wine oxidation, its assessment using EPR spin trapping, and potential mechanisms of chitosan protection. 4-MeC, 4-methylcatechol.

**Fig. 2.** Spin traps used in the study, spin adducts detected, and representative EPR spectra in the absence of inhibitor. Experimental conditions: (a) incubation of wine for 96 h at room temperature in darkness in the presence of 4-POBN (15 mM); (b) photolysis of H<sub>2</sub>O<sub>2</sub> (3% v/v in 0.5% acetic acid solution) in the presence of DMPO (3.33 mM); (c) nucleophilic addition of water in the presence of FeCl<sub>3</sub> (30 mg/L), CuSO<sub>4</sub> (12.5 mg/L) and DEPMPO (55 mM). The asterisk indicates the asymmetric carbon of DEPMPO. Open circles indicate lines from a minor DEPMPO carbon centered radical adduct.

**Fig. 3.** Effect of treatments on 4-POBN-1-HER spin adduct formation at room temperature during oxidation under air of (A) model wine, and (B) SO<sub>2</sub> free Chardonnay wine. Treatments and 100 μM of Fe(II) as the oxidant were first applied for 48 h, followed by addition of 4-POBN (15 mM) alone (real wine) or with 1 mM of 4-methylcatechol (model wine). Continuous agitation was applied throughout. CHI, chitosan. Level of significance vs. control (by one-way ANOVA followed by Duncan test): (A): \*\*p < 0.01 vs. CHI-2; \*p < 0.05 vs. CHI-2; §p < 0.05 vs. CHI-1 (all at any dose); (B): \*\*p < 0.01 vs. CHI-2 (any dose); #p < 0.05 vs. CHI-2 (2 g/L). Vertical bars represent SEM (n = 3–10).

**Fig. 4.** Effect of varying H<sub>2</sub>O<sub>2</sub> on the EPR signal detected in model wine 130 s (filled bars) or 10 min (empty bars) after induction of a Fenton reaction in the presence of wine-like concentrations of iron(II). The dashed line visualizes the maximum of spin adduct levels obtained in incubations (Fig. 3). Vertical bars represent SEM (n = 3).

**Fig. 5.** Assessment by EPR using various spin traps of the inhibitory effect of chitosan (CHI) on some potential mechanisms involved in wine oxidation. (A) Effect on [100  $\mu$ M Fe(II)/ 2.5  $\mu$ g/mL H<sub>2</sub>O<sub>2</sub>] Fenton reagent in model wine; (B) Determination of apparent rate constants for direct hydroxyl radical scavenging in acidic water (pH 3.17).  $I_0$ ,  $I$ : intensity of EPR signal in unsupplemented and test sample, respectively. Concentrations are estimates from mean molecular weights; (C) Inhibition of metal-catalyzed nucleophilic addition in water, in the presence of a wine-relevant metal concentration [30 mg/L of Fe(II) + 12.5 mg/L of Cu(II)]. Nitrones used were: (A) 4-POBN (15 mM); (B) DMPO (3.33 mM); and (C) DEPMPO (55 mM). Samples in A and C were pre-incubated with metals as described in the legend of Fig. 3. 4-MeC, 4-methylcatechol at 1 mM. Vertical bars represent SEM ( $n = 3$ ).

**Table 1**Radical scavenging activity and effect of treatments on spin adduct and fluorescent lightning induced acetaldehyde formation<sup>a,b</sup>.

sample and treatment	ORAC ( $\mu\text{mol Trolox/mL}$ )	AUC/incubation time <sup>c</sup>						acetaldehyde (mg/L)			
		1 day		2 days		3 days		control <sup>d</sup>	1 day	4 days	6 days
		Ctr	CHI-2 (2 g/L)	Ctr	CHI-2 (2 g/L)	Ctr	CHI-2 (2 g/L)				
MW <sup>e</sup>	not measurable										
MW + 4-MeC <sup>f</sup>	6.24 $\pm$ 0.27	11	5	47	18	99	31				
Chardonnay wine	3.18 $\pm$ 0.12	23	11	61	36	110	63	10.8 $\pm$ 0.4	14.1 $\pm$ 0.7***	16.2 $\pm$ 0.9***	21.6 $\pm$ 1.7***
+ CHI-2 (0.5 g/L)								10.0 $\pm$ 0.3	11.8 $\pm$ 0.5*§	13.0 $\pm$ 0.3*§	17.4 $\pm$ 1.2*§
+ CHI-2 (2 g/L)								9.6 $\pm$ 0.3§	10.3 $\pm$ 0.3 <sup>+</sup>	11.5 $\pm$ 0.3**	13.4 $\pm$ 1.0* <sup>+</sup>
+ SO <sub>2</sub> (50 mg/L)								5.0 $\pm$ 0.1§	5.4 $\pm$ 0.3 <sup>+</sup>	6.7 $\pm$ 0.5* <sup>+</sup>	11.2 $\pm$ 0.8* <sup>+</sup>

<sup>a</sup>. In the presence of 100  $\mu\text{M}$  of Fe(II).<sup>b</sup> Mean  $\pm$  SEM ( $n = 3-5$ ).<sup>c</sup> AUC, area-under-curve (arbitrary units) calculated from the curves in Fig. 3. Ctr, unsupplemented sample.

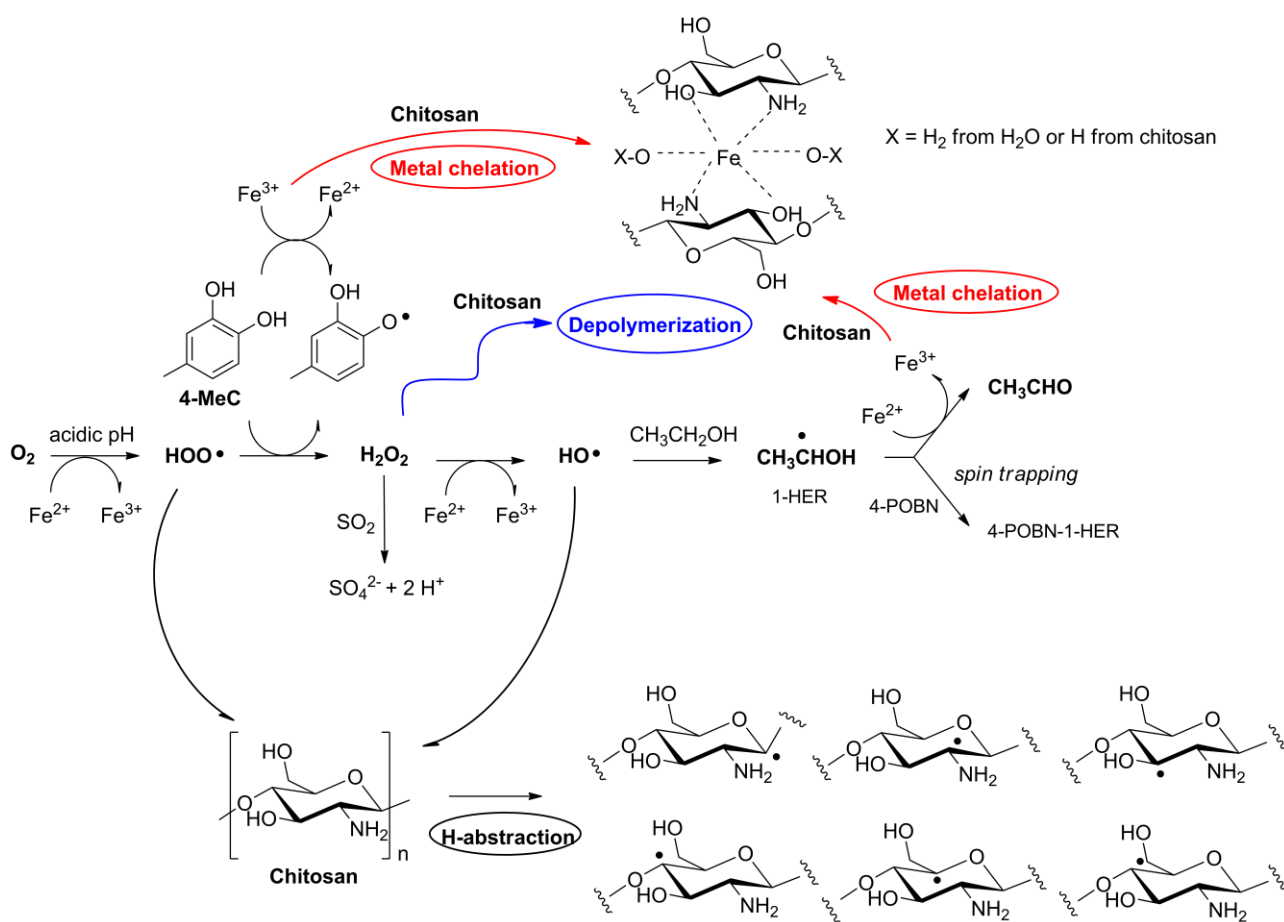
Table 1 (continued)

<sup>d</sup> Before illumination, after 2-days incubation in darkness.

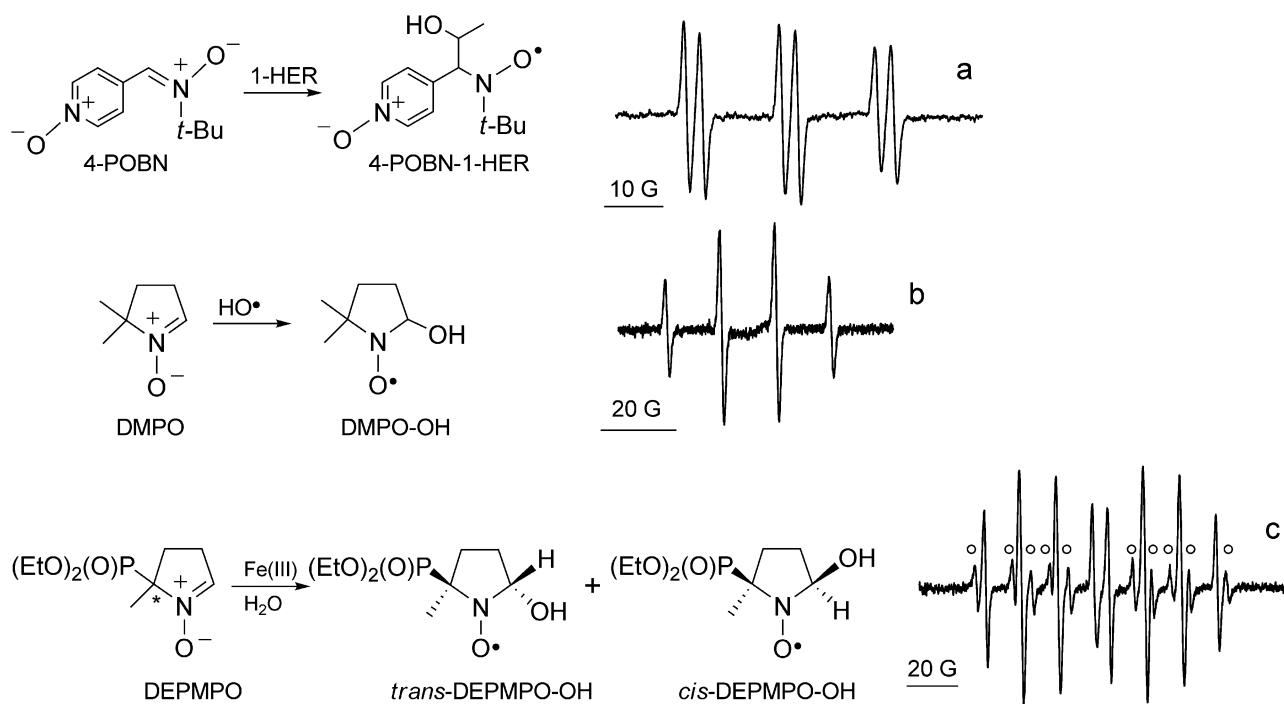
<sup>e</sup> Model wine (12% v/v, 8 g/L tartaric acid, pH 3.5).

<sup>f</sup> 4-methylcatechol at 1 mM.

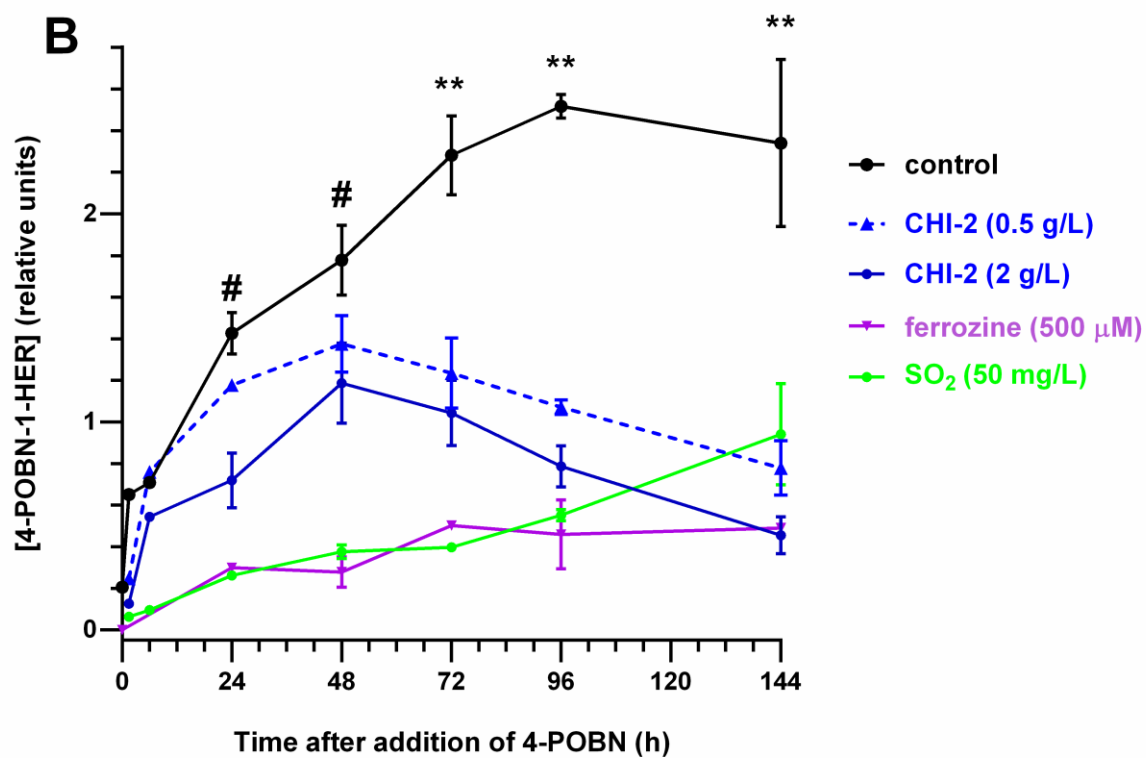
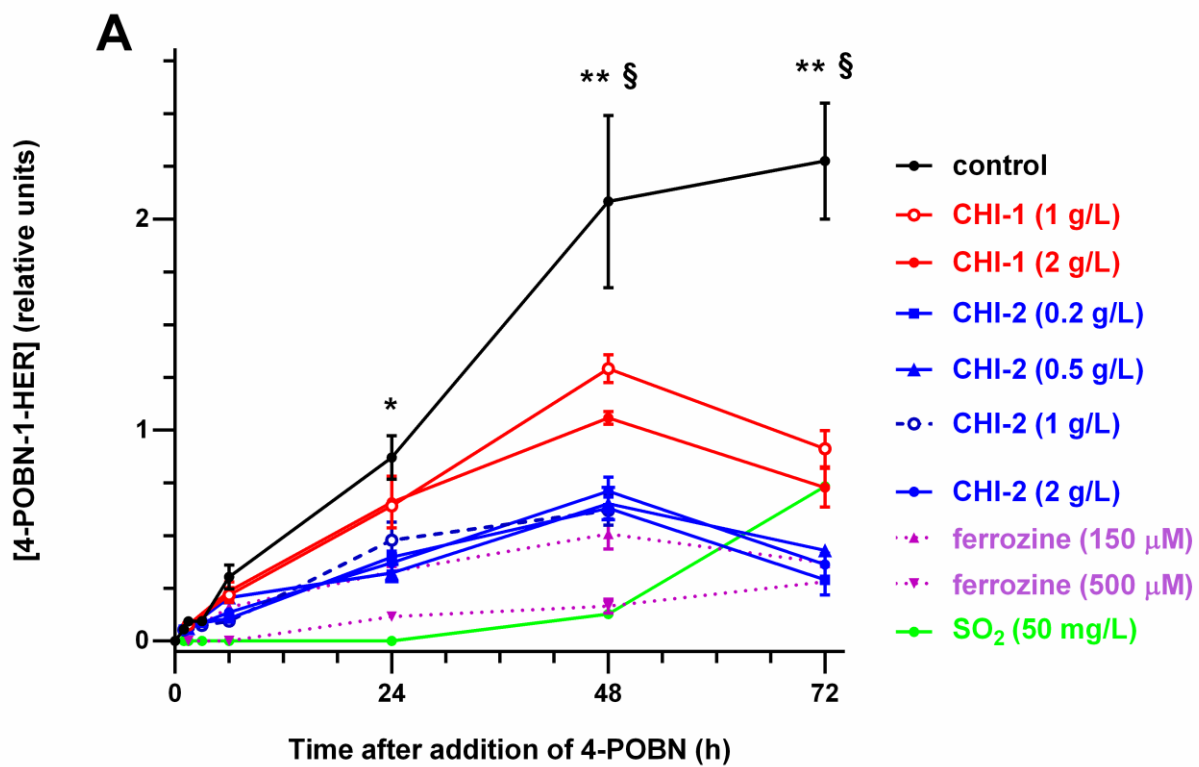
Statistics: (\*p < 0.05 and \*\*\*p < 0.001) vs. pre-illuminated control; (§p < 0.05 and †p < 0.001) vs. untreated wine after the same illumination time.

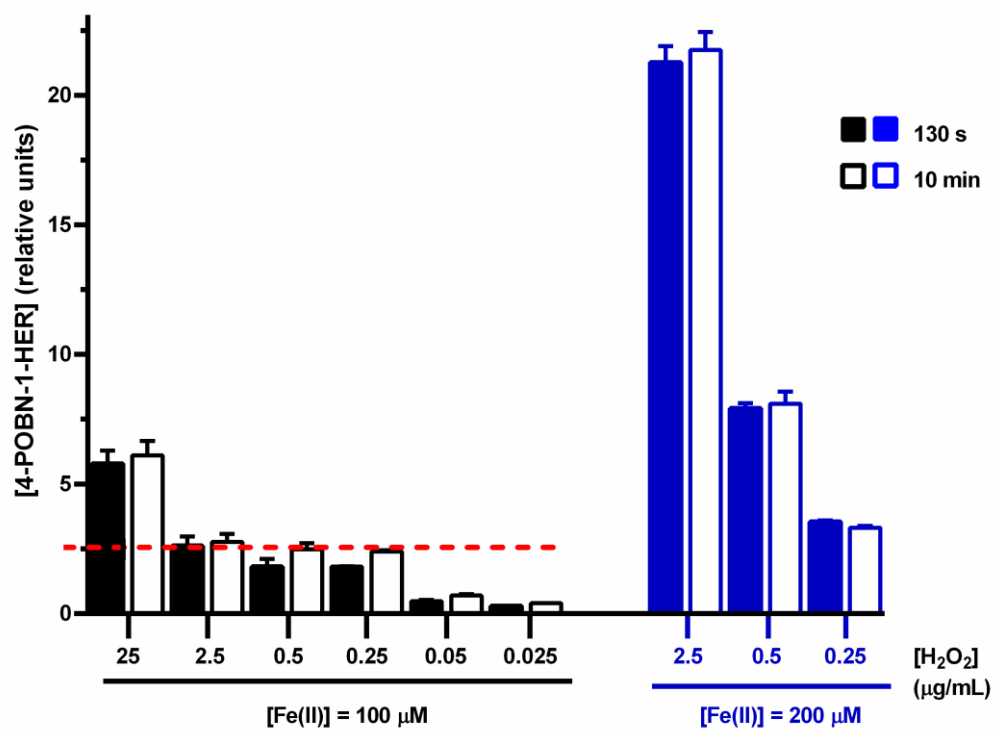


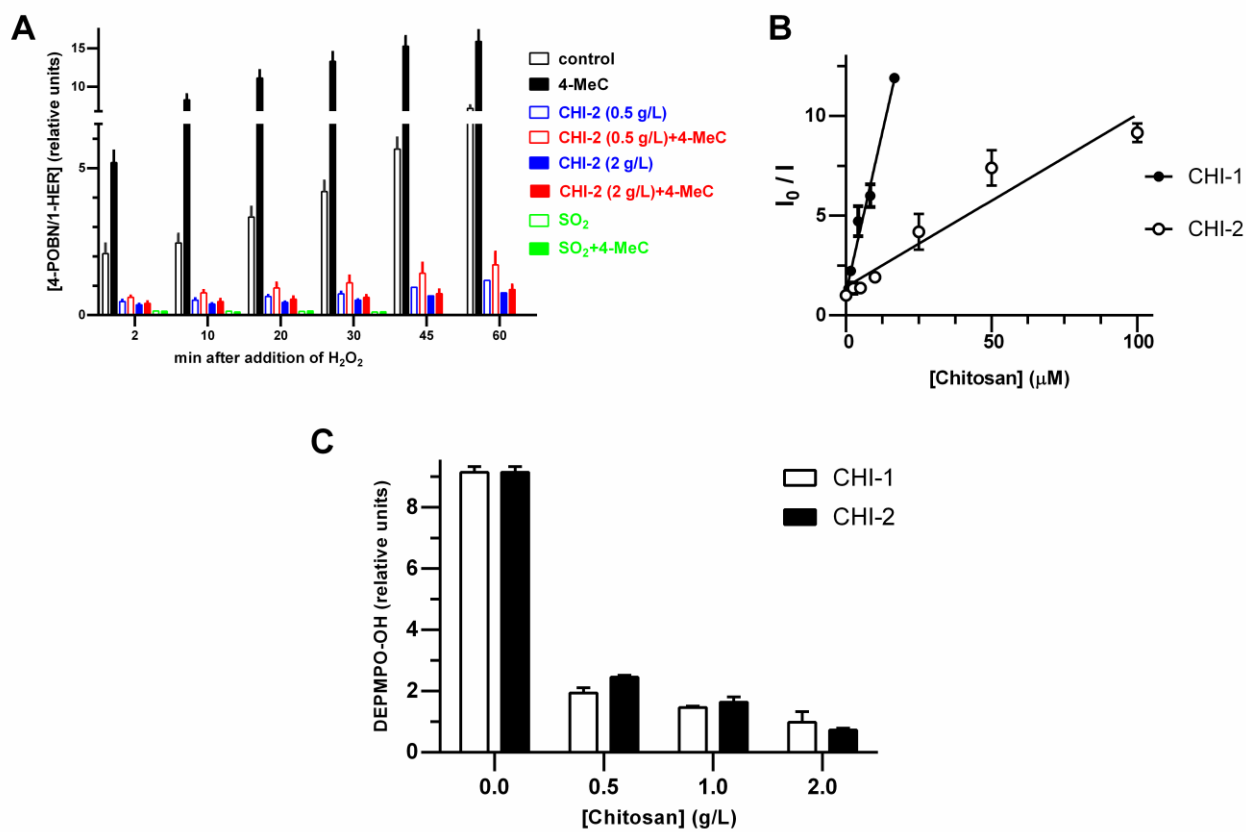
ACCEPTED



ACCEPTED







Metal chelation and free radical scavenging in wine oxidation were tested by EPR.

A dose of 2 g/L of approved chitosan efficiently stabilized an un sulphited white wine.

Inhibition of Fe(II)/Fenton chemistry and scavenging of hydroxyl radicals are involved.

Concomitant decreased acetaldehyde formation was observed.

ACCEPTED MANUSCRIPT